Gecko

Design for IGA-type discretization workflows

Gecko Technical Report 1

DC3 - Andrea Gorgi

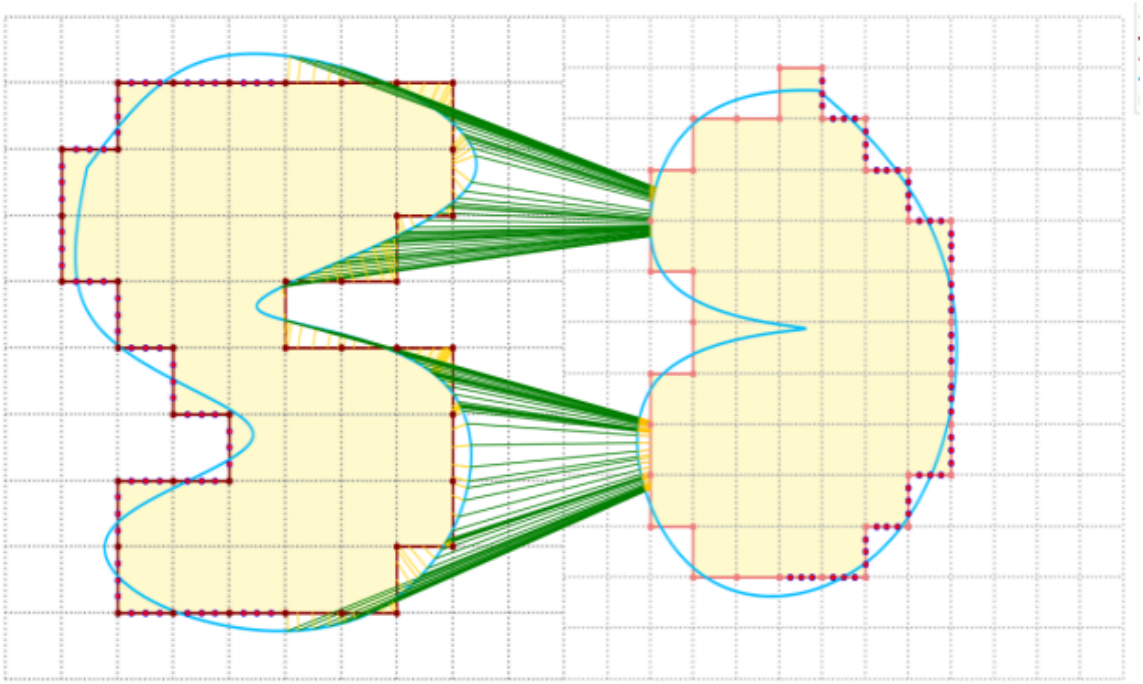

This project has received funding from the European Union's Horizon Europe research and innovation programme under grant agreement No 101073106
Call: HORIZON-MSCA-2021-DN-01

Funded by the European Union

Executive summary

This report presents the current state of the PhD project on immersed and high-order computational mechanics based on the Shifted Boundary Method (SBM) and Isogeometric Analysis (IGA). The original objective of the work was to combine the geometric flexibility of SBM with the high-order accuracy and smooth spline-based approximation of IGA, in order to address structural and contact mechanics problems on complex geometries more efficiently than standard body-fitted approaches. Within this general framework, particular attention has been devoted to weak imposition of boundary and interface conditions through Nitsche-type formulations, with the broader goal of enabling robust immersed simulations in the presence of contact, nonconforming geometries, and localized features.

The project has now evolved along two main research lines. The first is immersed contact mechanics, where an SBM-based formulation for frictionless contact in linear elasticity has been developed, in collaboration with Kangan Li and Guglielmo Scovazzi [47], and validated through two- and three-dimensional benchmark problems and complex non-watertight geometries. At present, however, this contribution has been achieved in the FEM setting, effectively for low-order discretizations, while the extension to high-order IGA is still under development.

The second, and currently central, contribution is the development of the high-order isogeometric Gap–SBM. This formulation was introduced to overcome one of the main limitations of the classical SBM, namely the reduced accuracy in the treatment of Neumann boundary conditions. Instead of neglecting the region between the surrogate and true boundaries, the Gap–SBM explicitly reconstructs its contribution through high-order Taylor extensions and curvilinear gap elements, achieving optimal convergence for both Dirichlet and Neumann conditions without introducing additional degrees of freedom and while preserving favorable conditioning. This also makes the formulation structurally suitable for future extensions to nonlinear constitutive behavior, including plasticity.

Another relevant contribution is a multipatch coupling framework based on Gap–SBM. Although this is a more methodological development, it is highly relevant for the overall project because it enables robust coupling of nonconforming patches with different parametrizations, mesh sizes, and polynomial orders, without requiring watertight interfaces or matching knot vectors. Most importantly, it provides a simple and flexible way to introduce local refinement near critical regions of the domain, which is expected to be especially useful for immersed contact and, more generally, for problems involving localized gradients, non-smooth responses, or evolving nonlinear zones.

Taken together, these results shift the project from the initial proof of concept of combining SBM and IGA toward a more mature framework in which immersed contact, accurate Neumann treatment, and local adaptive refinement are progressively being unified. The next steps are therefore to compare immersed contact formulations based on the classical SBM and the Gap–SBM, supported by local refinement strategies, and then to extend the same comparison to nonlinear materials and plasticity, with the long-term aim of addressing contact problems involving more complex physics.

List of abbreviations

ALM	*Augmented Lagrangian Multiplier method*
FEM	*Finite Element Method*
IGA	*IsoGeometric Analysis*
LM	*Lagrangian Multiplier method*
SBM	*Shifted Boundary Method*

Introduction

Isogeometric Analysis (IGA) has established itself as a powerful framework in computational mechanics by bridging the gap between Computer-Aided Design (CAD) and numerical simulation. By employing spline-based basis functions such as B-splines and NURBS, IGA enables exact geometry representation, high-order accuracy, and enhanced continuity across element interfaces, often achieving superior accuracy per degree of freedom compared with standard finite element discretizations. These properties are especially attractive in structural and contact mechanics, where geometric fidelity and smooth stress representation play a central role.

Despite these advantages, the practical use of boundary-fitted IGA remains challenging for complex geometries, trimmed models, and nonconforming interfaces. The generation of analysis-suitable parametrizations may require substantial preprocessing, while immersed and embedded approaches based on cut-cell integration are often affected by the small cut-cell problem, which can lead to poor conditioning and increased algorithmic complexity. Within this context, the Shifted Boundary Method (SBM) provides an attractive alternative by replacing the true boundary with a surrogate boundary aligned with the background mesh and transferring the boundary conditions through Taylor expansions. In this way, SBM avoids cut-cell integration, simplifies preprocessing, and preserves the favorable conditioning properties of the discretization. Its integration within IGA has therefore opened a promising route toward accurate and flexible high-order immersed simulations on complex domains.

The initial stage of this work focused on this integration of SBM within IGA and on its application to contact mechanics through a penalty-free Nitsche formulation. In the previous technical report, this framework was validated on classical benchmarks such as the patch test, the Hertz contact problem, and the punch test, showing that accurate and robust contact enforcement could be achieved without introducing Lagrange multipliers or penalty parameters. These results established the basis for extending the overall methodology toward immersed contact mechanics.

Since then, the project has evolved in two closely connected directions. On the one hand, in collaboration with Kangan Li and Guglielmo Scovazzi, an immersed SBM formulation for contact in linear elasticity has been developed and validated in the FEM setting [47], demonstrating that contact conditions can be imposed on surrogate contact surfaces while retaining robustness and avoiding cut-cell integration, even for complex and non-watertight geometries. On the other hand, the main methodological effort has shifted toward the development of the high-order isogeometric Gap–Shifted Boundary Method (Gap–SBM), introduced to overcome one of the main limitations of the classical SBM, namely the reduced accuracy in the treatment of Neumann boundary conditions. By explicitly accounting for the region between the surrogate and true boundaries through high-order Taylor extensions and gap integration, the Gap–SBM restores optimal convergence for both Dirichlet and Neumann conditions without adding degrees of freedom and while maintaining favorable numerical conditioning.

Within this same line of development, another contribution is a multipatch coupling strategy derived from the Gap–SBM framework. In the context of the present project, this should mainly be regarded as an enabling tool, since it allows nonconforming patches with different parametrizations, mesh sizes, and polynomial orders to be coupled in a robust way, while also making local refinement near critical regions significantly easier to introduce. This added flexibility is expected to play an important role in the next stages of the research, particularly for

a more accurate comparison between classical SBM and Gap–SBM in immersed contact, and for future extensions to nonlinear materials and plasticity.

1. The Shifted Boundary Method in IGA

Isogeometric Analysis (IGA) has emerged as a transformative approach in computational mechanics, bridging the longstanding gap between Computer-Aided Design (CAD) and Computer-Aided Engineering (CAE). Initially proposed by Hughes et al. [1, 2, 3, 4, 5], IGA delivers precise geometric representations and high levels of continuity at element interfaces [6], making it especially effective for accurately modeling intricate geometries [7, 8, 9]. The foundation of IGA lies in employing B-Splines and NURBS basis functions, which provide smooth transitions and enable localized refinements, ultimately enhancing the reliability and precision of simulations [10, 11].

Despite its strengths, traditional boundary-fitted implementations of IGA encounter notable hurdles with complex geometries. These include the need for watertight models and the computational overhead of managing trimmed or discontinuous surfaces [12, 13]. To address these challenges, immersed boundary techniques, such as the Finite Cell Method (FCM) [14, 15] and Isogeometric Boundary Representation Analysis (IBRA) [16, 17, 18, 19, 20], have been introduced. These methods bypass the need for strict boundary conformity by working with non-boundary-fitted meshes. However, a persistent issue in these approaches is the handling of small cut cells [21, 22], which can degrade computational performance and complicate solver convergence.

The Shifted Boundary Method (SBM) [23,24], originally developed in the context of the Finite Element Method (FEM), provides an innovative approach to overcoming challenges associated with traditional boundary-fitted methods. By shifting boundary conditions to a surrogate boundary and leveraging Taylor expansions for accurate boundary value modifications, SBM effectively eliminates the issues caused by small cut-cells. This simplification not only maintains optimal accuracy but also reduces the complexity of mesh generation and refinement. Applications of SBM in FEM have already demonstrated its efficacy in elasticity and incompressible fluid dynamics [25,26,27,28].

A brief comparison: IGA and FEM

A key step in advancing the use of IGA was the implementation of a general body-fitted problem, where a flexible, nonlinear mapping between the parameter and physical spaces was developed. This mapping leverages IGA's inherent capability to describe CAD geometries perfectly, ensuring precise simulation of even the most complex domains.

Advantages of IGA over FEM in Body-Fitted Scenarios

Comparative studies between IGA and FEM have revealed several advantages of IGA in body-fitted scenarios:

1. **Reduced Degrees of Freedom (DOFs)**:
   IGA requires fewer DOFs to achieve the same error level compared to FEM. This is due to the higher-order continuity of NURBS, which reduces the number of elements and control points needed for accurate approximations.
2. **Exact Geometry Representation**:
   Unlike FEM, where mesh generation can introduce geometric inaccuracies, IGA

ensures that the computational domain is an exact replica of the CAD model (Figure 1). This exactness is particularly beneficial for problems where geometric fidelity is critical, such as those involving contact mechanics.

3. **Simplified Refinement**:
   Refinement in IGA can be achieved without altering the underlying geometry, making it more straightforward to adapt the computational model to different levels of precision.
4. **Higher Convergence Velocity**:
   Both FEM and IGA exhibit similar convergence orders when using the same polynomial degree. However, IGA's ability to easily increase the order of basis functions without remeshing provides a significant edge. Higher-order basis functions lead to enhanced convergence rates, enabling IGA to achieve desired accuracy more efficiently and lower numbers of degrees of freedom (Figure 2).

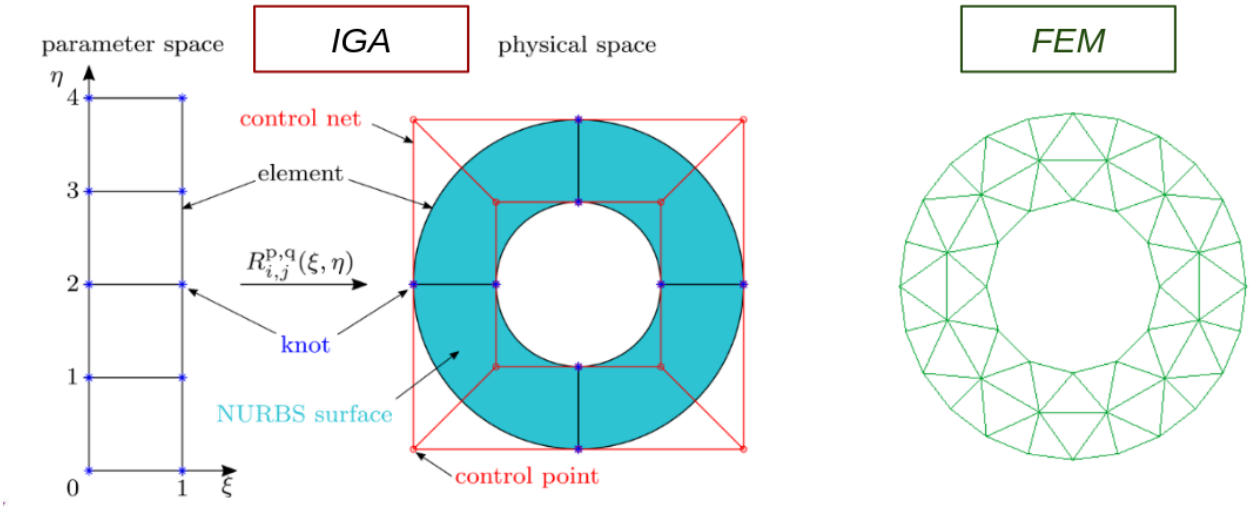

***Figure 1**. Comparison of IGA and FEM discretizations.*

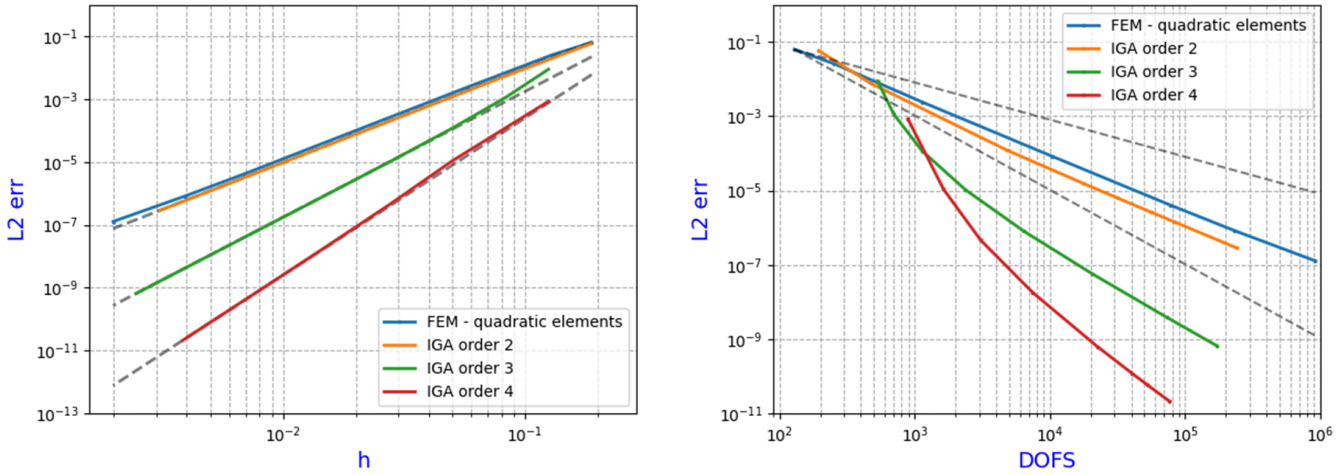

***Figure 2**. Comparison of IGA and FEM convergence and DOFs utilization.*

The Shifted Boundary Method

The Shifted Boundary Method (SBM) offers a flexible framework to address challenges in numerical integration over complex domains, including contact mechanics. As outlined in [29], SBM shifts the imposition of boundary conditions from the true boundary Γ to a surrogate boundary Γ_h, composed of edges of a computational grid.

Boundary conditions are modified using Taylor expansions, ensuring optimal convergence rates. This approach avoids challenges associated with small cut cells and simplifies numerical integration, making it particularly suited for embedded methods and large deformation problems.

In this context, the SBM complements Isogeometric Analysis (IGA) by leveraging exact geometry descriptions and avoiding trimmed knot spans. This synergy improves the representation of physical geometries and enhances computational efficiency.

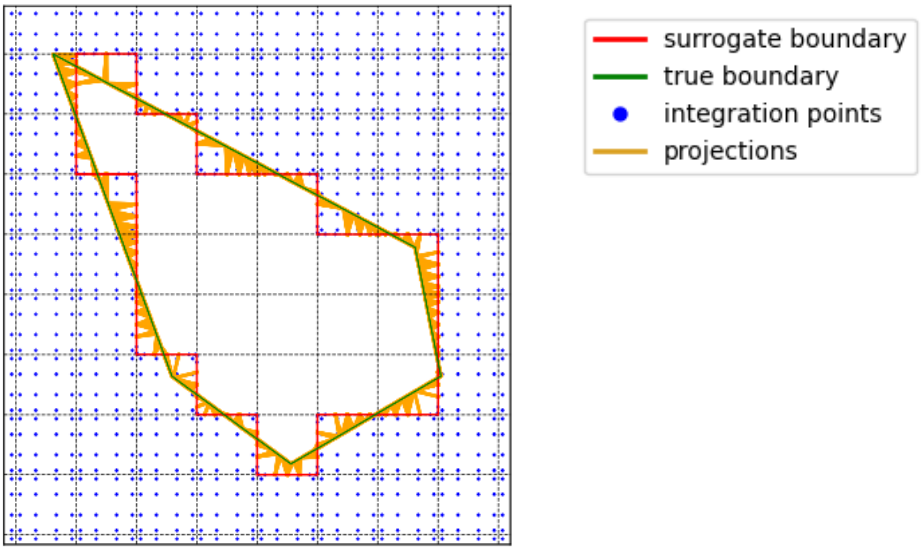

Figure 3: *SBM main characteristics.*

The SBM for IGA has been implemented inside the Kratos Multiphysics framework (KratosMultiphycsGithub) to handle 2D fluid and structural mechanics problems with complex geometries.

The SBM implementation preserves the optimal convergence of body-fitted cases under Dirichlet boundary conditions, though it experiences a one-order reduction in convergence for Neumann (load) conditions. This functionality has also been extended to 3D problems, broadening its applicability (Figure 4).

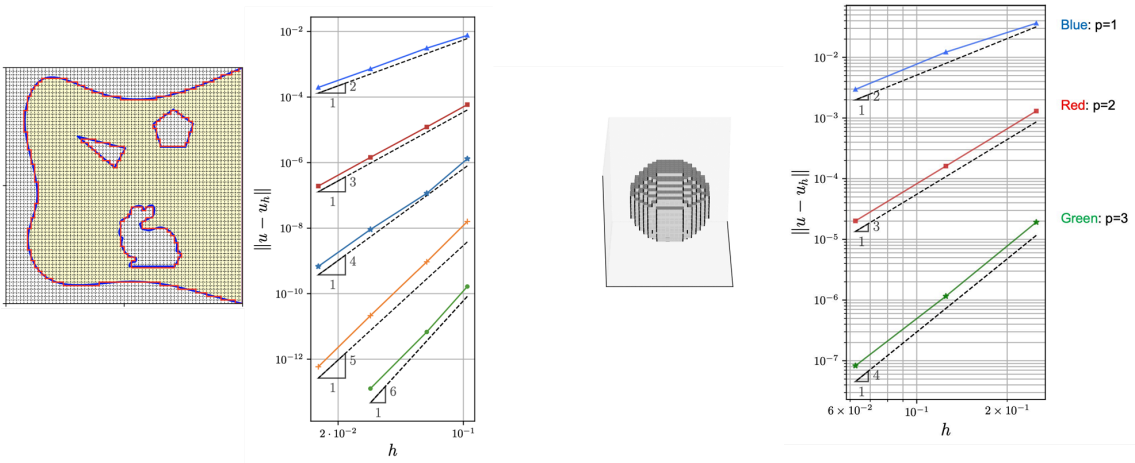

Figure 4. *IGA+SBM for 2D/3D problems.*

Finally, Figure 5 shows a convergence comparison between standard IGA and IGA with SBM for the case of circular geometry. No big loss is evident for the use of the SBM against the exact geometry of the body-fitted scenario.

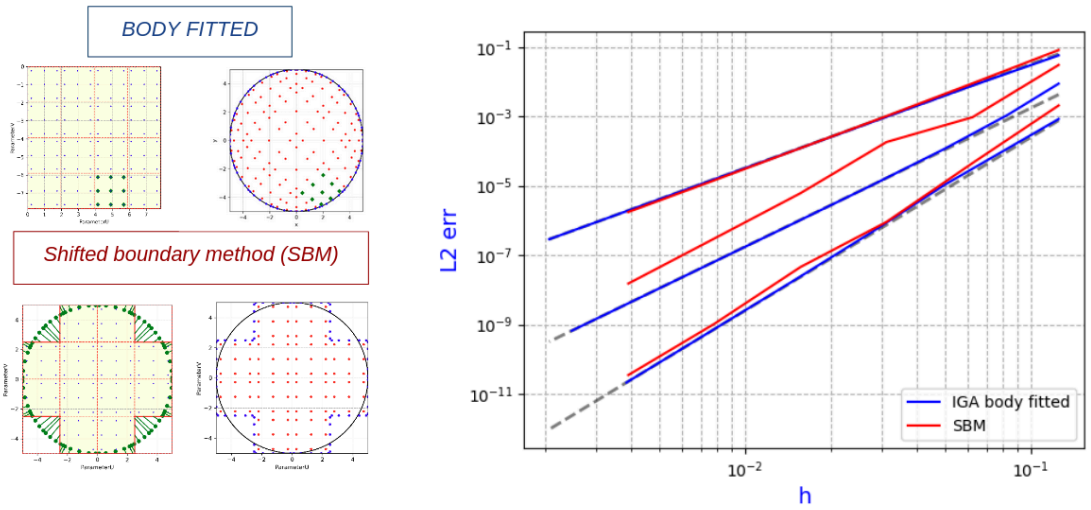

Figure 5. *Comparison of IGA body-fitted and IGA + SBM convergence for a circle.*

2. The Shifted Boundary Method for contact problems

The results summarized in this section were obtained in collaboration with Kangan Li and Guglielmo Scovazzi and are documented in [47]. We propose an embedded algorithm for contact mechanics based on the Shifted Boundary Method. The contact conditions are applied on a surrogate contact surface in proximity of the true contact surface and Taylor expansions are used to change (shift) both their value and location. This approach is robust, accurate, and avoids integrating the variational formulation on cut cells and related numerical instabilities. Computational experiments in both two and three dimensions are provided to demonstrate the performance of our methodology. The proposed approach offers an advantage whenever bodies of very complex shape come into contact, especially when the shapes are not represented using standard Computer Aided Design (CAD) formats. In all these situations, body-fitted grid generation may become extremely time consuming or completely unfeasible. The work presented here applies to frictionless contact under the hypothesis of small-strain contact mechanics, although the concepts are in principle extendable also to wider contexts.

The momentum balance equation in the physical domain Ω reads

$$\nabla \cdot \boldsymbol{\sigma}(\boldsymbol{u}) + \boldsymbol{f} = \boldsymbol{0}$$

where u is the displacement, f is the body force per unit volume, $\sigma(u)$ is the stress tensor and ∇ and $\nabla\cdot$ are the gradient and divergence operators, respectively. In particular $u = x - x_0$, that is the displacement is the difference between the current position of a material point and its original position x_0.

Let the boundary be partitioned into $\Gamma = \Gamma_D U \Gamma_N U \Gamma_C$, *as in Figure 6, where* Γ_C *is the candidate contact boundary. THe boundary conditions on* Γ_D *and* Γ_N *are, respectively,*

$$\boldsymbol{u} = \boldsymbol{u}_D \ , \quad \text{on } \Gamma_D \ ,$$
$$\boldsymbol{\sigma}(\boldsymbol{u})\boldsymbol{n} = \boldsymbol{t}_N \ , \quad \text{on } \Gamma_N \ ,$$

where t_N *is the normal traction and* n *is the outward-pointing normal to the bo*undary Γ . The boundary is further partitioned as $\Gamma_C = \Gamma_C^a \cup \Gamma_C^i$, where the apices “a” and “i” stands for active and inactive part of the contact boundary, respectively.

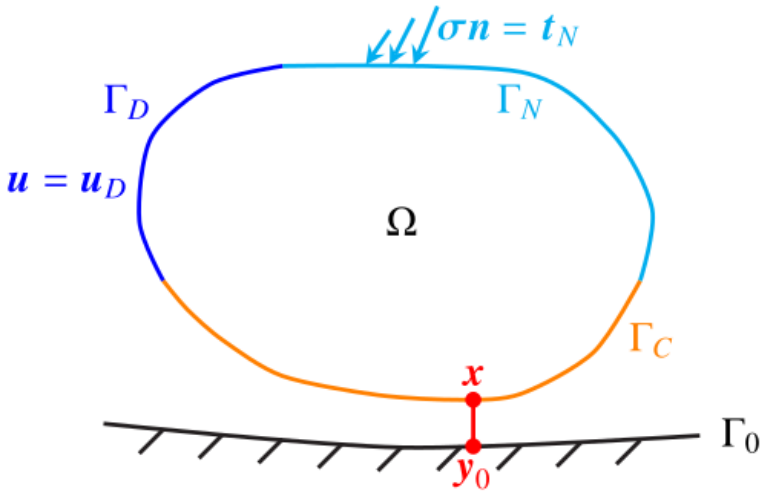

Figure 6. *Signorini’s problem: the domain and the boundary partition* $\Gamma = \Gamma_D U \Gamma_N U \Gamma_C$ *, with* $\Gamma_D \cap \Gamma_N = \varnothing$, $\Gamma_C \cap \Gamma_N = \varnothing$, *and* $\Gamma_D \cap \Gamma_C = \varnothing$.

The obstacle is represented as a curve/surface Γ_0 in the two/three-dimensional space, and a point x on Γ_C will come in contact with a corresponding candidate contact point $y_0 \in \Gamma_0$. The location of y_0 is typically found by means of closest-point projection techniques. One can define the normal gap between Γ_C and Γ_0 :

$$g_n(u) = (y_0 - x) \cdot n = (y_0 - x_0 - u) \cdot n = \underbrace{(y_0 - x_0) \cdot n}_{g_{n;0}} - u \cdot n,$$

Where n is the unit normal to Γ_C and $g_{n;0}$ the initial gap. This work is developed under the hypothesis of small-strain contact mechanics. Hence n and y_0 depend on the initial geometry and are kept fixed during simulations. The contact pressure is considered when $g_n(u(x)) = 0$, whereas on the inactive contact boundary Γ_C^i, instead, we have $g_n(u(x)) > 0$, and a traction-free condition is applied.

Now, the goal of the SBM is to modify the contact conditions so that they are applied on $\tilde{\Gamma}_C$ rather than Γ_C. For this reason we have introduced the shift operators that approximates the exact expansion values of $u(x)$ and $\sigma(x)$ on Γ_C:

$$\boldsymbol{S}(\boldsymbol{u})(\tilde{\boldsymbol{x}}) := \boldsymbol{u}(\tilde{\boldsymbol{x}}) + (\nabla \boldsymbol{u}\, \boldsymbol{d})(\tilde{\boldsymbol{x}}) ,$$
$$\boldsymbol{S}(\boldsymbol{\sigma}(\boldsymbol{u}))(\tilde{\boldsymbol{x}}) := \boldsymbol{\sigma}(\boldsymbol{u}(\tilde{\boldsymbol{x}})) + (\nabla \boldsymbol{\sigma}(\boldsymbol{u})\, \boldsymbol{d})(\tilde{\boldsymbol{x}}).$$

We can henceforth redefine the normal gap by means of this shift operator as:

$$g_n(\boldsymbol{S}(\boldsymbol{u})) = g_{n;0} - \boldsymbol{S}(\boldsymbol{u}) \cdot \boldsymbol{n} = g_{n;0} - (\boldsymbol{u} + \nabla \boldsymbol{u}\boldsymbol{d}) \cdot \boldsymbol{n}.$$

A convenient way to summarize the derivation is to start from the classical body-fitted Signorini problem and use the Lagrange multiplier only as a conceptual bridge to the final primal formulation. In the body-fitted setting, unilateral frictionless contact can be described in terms of the normal gap $g_n(u)$ and of the normal contact traction λ_n, subject to the Hertz-Signorini-Moreau conditions

$$\lambda_n \leq 0\,, \qquad g_n \geq 0\,, \qquad \lambda_n\, g_n = 0$$

An augmented multiplier can then be introduced as $\tilde{\lambda}_n := \lambda_n + \alpha g_n(u)$ that the active and inactive contact regions are identified by the sign of $\tilde{\lambda}_n$. This construction is useful because it provides a robust framework for the treatment of the transition between contact and no-contact [47].

In the shifted-boundary setting, however, the derivation is not obtained by writing a shifted potential functional. Instead, the formulation is derived directly from the strong form of linear elasticity posed on the surrogate domain, after testing it with admissible variations and replacing the contact conditions on the true boundary with their shifted counterparts on the surrogate contact boundary.
For this reason we have introduced the shift operators that approximates the exact expansion values of $u(x)$ and $\sigma(x)$ on Γ_C:

$$\boldsymbol{S}(\boldsymbol{u})(\tilde{\boldsymbol{x}}) := \boldsymbol{u}(\tilde{\boldsymbol{x}}) + (\nabla \boldsymbol{u}\, \boldsymbol{d})(\tilde{\boldsymbol{x}}) ,$$
$$\boldsymbol{S}(\boldsymbol{\sigma}(\boldsymbol{u}))(\tilde{\boldsymbol{x}}) := \boldsymbol{\sigma}(\boldsymbol{u}(\tilde{\boldsymbol{x}})) + (\nabla \boldsymbol{\sigma}(\boldsymbol{u})\, \boldsymbol{d})(\tilde{\boldsymbol{x}}).$$

We can henceforth redefine the normal gap by means of this shift operator as:

$$g_n(\boldsymbol{S}(\boldsymbol{u})) = g_{n;0} - \boldsymbol{S}(\boldsymbol{u}) \cdot \boldsymbol{n} = g_{n;0} - (\boldsymbol{u} + \nabla \boldsymbol{u}\boldsymbol{d}) \cdot \boldsymbol{n}.$$

and the corresponding shifted augmented multiplier as

$$\tilde{\lambda}_n := \lambda_n + \alpha g_n(\boldsymbol{S}(\boldsymbol{u}))$$

The active and inactive portions of the surrogate contact boundary are then identified by the signs of this new $\tilde{\lambda}_n$. This allows the contact conditions to be consistently transferred from the true boundary to the surrogate one.

Starting from the weak form of the momentum balance on the surrogate domain and inserting the shifted contact conditions, one obtains the shifted augmented formulation. In compact form, its structure can be written as

$$(\varepsilon(v), C\varepsilon(u))_{\tilde{\Omega}} - \langle v, \sigma(u)\tilde{n} - (\tilde{n}\cdot n)S(\sigma(u))n\rangle_{\tilde{\Gamma}_C} - \langle (\tilde{n}\cdot n)v, (\lambda_n + \gamma g_n(S(u)))n\rangle_{\tilde{\Gamma}_C^a}$$
$$+\langle (\tilde{n}\cdot n)\mu_n, g_n(S(u))\rangle_{\tilde{\Gamma}_C^a} - \langle (\tilde{n}\cdot n)\mu_n, \gamma^{-1}\lambda_n\rangle_{\tilde{\Gamma}_C^i} = (v, f)_{\tilde{\Omega}} + \langle v, t_N\rangle_{\Gamma_N}.$$

Here, the factor $(\tilde{n}\cdot n)$ accounts for the geometric relation between surrogate and true boundaries. The shifted Nitsche formulation is finally obtained by replacing the Lagrange multiplier with the shifted normal stress, namely

$$\lambda_n = n\cdot(S(\sigma(u))n), \qquad \mu_n = n\cdot(S(\sigma(v))n).$$

In this way, the formulation becomes purely primal and no additional multiplier unknown is required. The skew-symmetric Nitsche variant adopted in the paper can be written as

$$(\varepsilon(v), C\varepsilon(u))_{\tilde{\Omega}} - \langle v, \sigma(u)\tilde{n} - (\tilde{n}\cdot n)S(\sigma(u))n\rangle_{\tilde{\Gamma}_C}$$
$$-\langle (\tilde{n}\cdot n)(v\cdot n),\, n\cdot(S(\sigma(u))n) + \gamma g_n(S(u))\rangle_{\tilde{\Gamma}_C^a} - \langle (\tilde{n}\cdot n)\, n\cdot(S(\sigma(v))n),\, g_n(S(u))\rangle_{\tilde{\Gamma}_C^a}$$
$$+\langle (\tilde{n}\cdot n)\, n\cdot(S(\sigma(v))n),\, \gamma^{-1} n\cdot(S(\sigma(u))n)\rangle_{\tilde{\Gamma}_C^i} = (v, f)_{\tilde{\Omega}} + \langle v, t_N\rangle_{\Gamma_N}.$$

Therefore, the final SBM contact formulation is obtained by combining the shifted description of the contact kinematics with a Nitsche treatment of the contact traction, leading to an immersed formulation that avoids cut-cell integration while preserving robustness and consistency.

2.1 Numerical Results

To test the developed formulation we test it with a well-known benchmark, in which a half-disk comes into contact with a rigid horizontal wall (Signorini's problem). This test simulates Hertzian-type contact and is widely adopted in the literature [48].

The geometry is depicted in Fig. 7 with R = 8 mm. Two traction boundary conditions of type $t_n = (0, -p_N)$ are considered, with = 0.1 GPa and 0.3 GPa, respectively. Note that only half of the geometry (the light gray region in Fig. 7) is modeled, due to symmetry. Young's modulus

is E = 200 GPa and Poisson's ratio is $\nu = 0.3$. The analytical contact pressure on is described by the classical Hertzian solution:

$$p_c = \frac{4Rp_N}{\pi b^2}\sqrt{b^2 - x^2}\,, \quad \text{with} \quad b = 2\sqrt{\frac{2R^2p(1-\nu^2)}{E\pi}}\,,$$

where denotes the width of the contact zone.

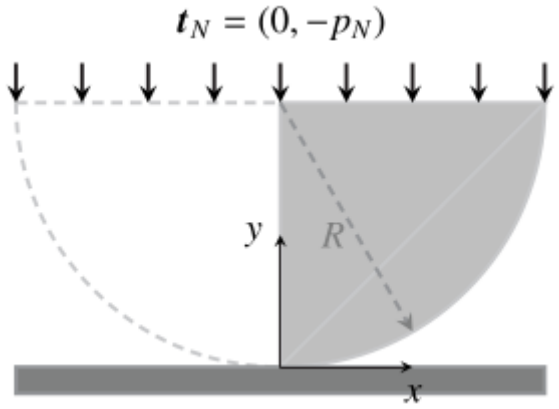

Figure 7. *Two-dimensional Hertzian contact problem with circular boundary: geometry and setup.*

The body-fitted and SBM simulation are performed over six computational grids each, described in Table 1.

Table 1
Two-dimensional Hertzian contact problem with circular boundary. Properties of the meshes: body-fitted meshes (B1, B2, B3, etc.) and embedded SBM meshes (E1, E2, E3, etc.).

	Body-fitted mesh						SBM (Embedded) mesh					
	B1	B2	B3	B4	B5	B6	E1	E2	E3	E4	E5	E6
No. elements	1185	4740	18,960	75,840	303,360	1,213,440	1066	4338	17,509	70,384	282,243	1,130,283
No. nodes	638	2460	9659	38,277	152,393	608,145	579	2261	8940	35,563	141,863	566,624

The Hertz disk-wall benchmark shows that the primal SBM formulation is able to reproduce the body-fitted solution with very good accuracy. As observed in the displacement and von Mises stress contours, the numerical fields obtained with the two approaches are nearly indistinguishable, indicating that the shifted treatment of the contact boundary does not introduce visible distortions in either the global deformation pattern or the stress distribution (see Figure 8).

A similarly good agreement is observed in the contact pressure distribution along the contact boundary. The primal SBM results recover the classical Hertzian profile and converge to the analytical solution under mesh refinement, with an accuracy comparable to the body-fitted formulation. On the finest grids, the error in the maximum contact pressure remains below 1% for all formulations considered; more specifically, the body-fitted solution shows a slight

overestimation, whereas the primal SBM produces a slight underestimation. Overall, these results show that the SBM formulation provides an accurate and robust immersed treatment of Hertzian contact, while retaining the main features of the body-fitted reference solution.

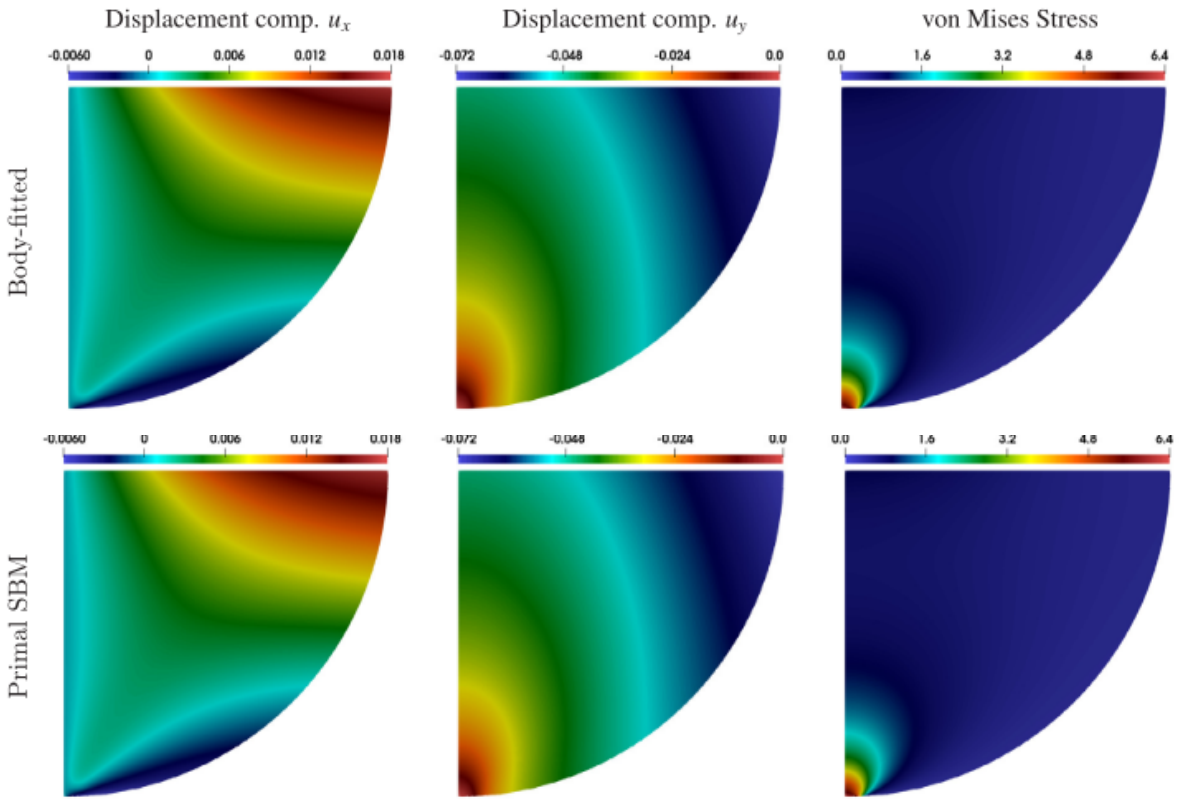

Figure 8. *Two-dimensional Hertzian contact problem with circular boundary* p_N *= 0.3 GPa: displacement components (x and y) and the von Mises stress with the body-fitted and SBM formulation.*

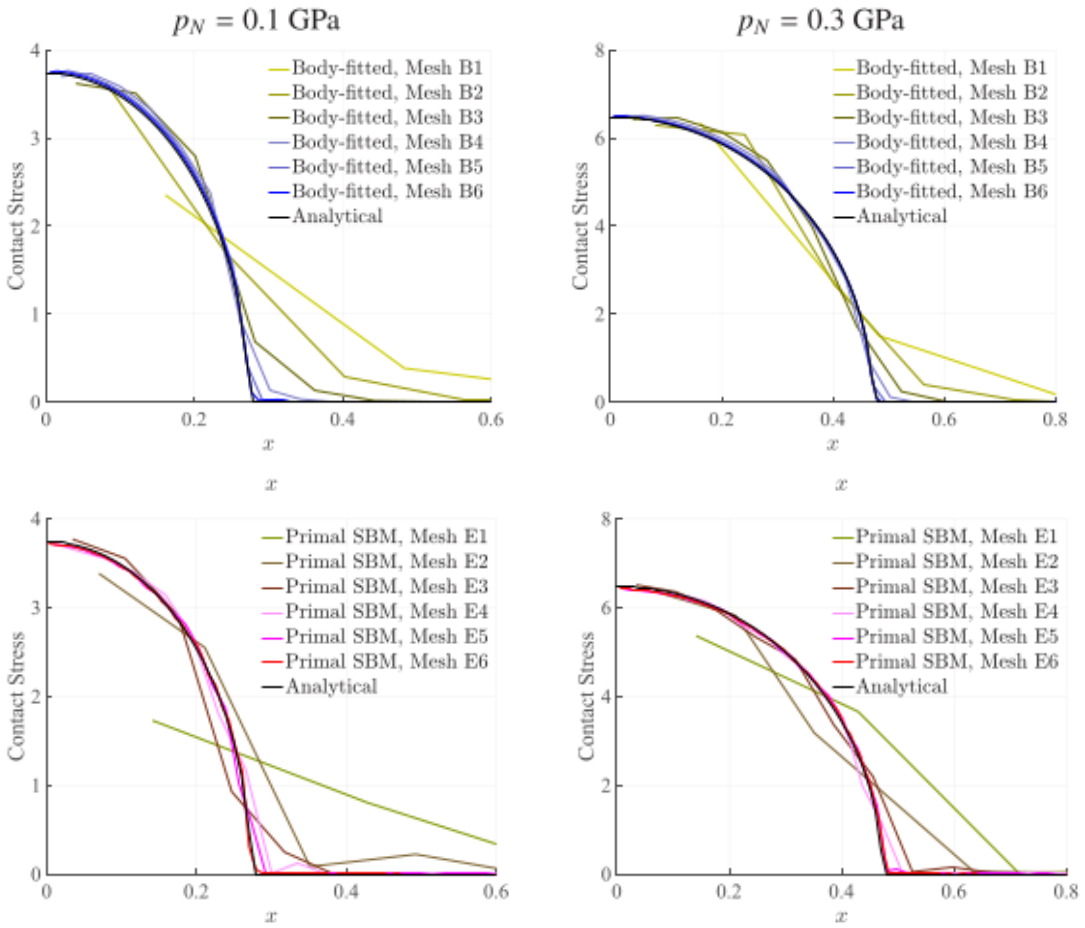

Figure 9. *Two-dimensional Hertzian contact problem with circular boundary (for p_N= 0.1 GPa and p_N= 0.3 GPa): contact pressure along the boundary .*

The formulation was also extended to two-body problems and in three dimensions.

3. The Gap Shifted Boundary Method in IGA

This work [49] introduces a high-order isogeometric extension of the Gap–Shifted Boundary Method for linear elasticity, aimed at overcoming some of the main limitations of standard immersed high-order approaches. The key idea is to explicitly account for the gap between the surrogate and true boundaries by extending the spline approximation into the gap region through high-order Taylor expansions and by reconstructing its contribution with curvilinear gap elements. In this way, the method avoids cut-cell integration, preserves favorable conditioning, and restores accurate imposition of Neumann boundary conditions without adding extra degrees of freedom. Numerical results show optimal convergence for both Dirichlet and Neumann conditions, limited sensitivity to the surrogate boundary position, and good robustness even for geometries with features much smaller than the background mesh size.

The key idea of the Gap–SBM is to explicitly account for the geometric gap between the surrogate and true boundaries, instead of neglecting it as in the classical SBM. This is achieved by extending the active B-spline approximation into the gap region through high-order Taylor expansions and by reconstructing the contribution of the gap through curvilinear gap elements, built in a way that is geometrically consistent with the polynomial degree of the discretization (see figures 10 and 11). Since these gap elements are introduced only for integration purposes, no additional degrees of freedom are added to the problem.

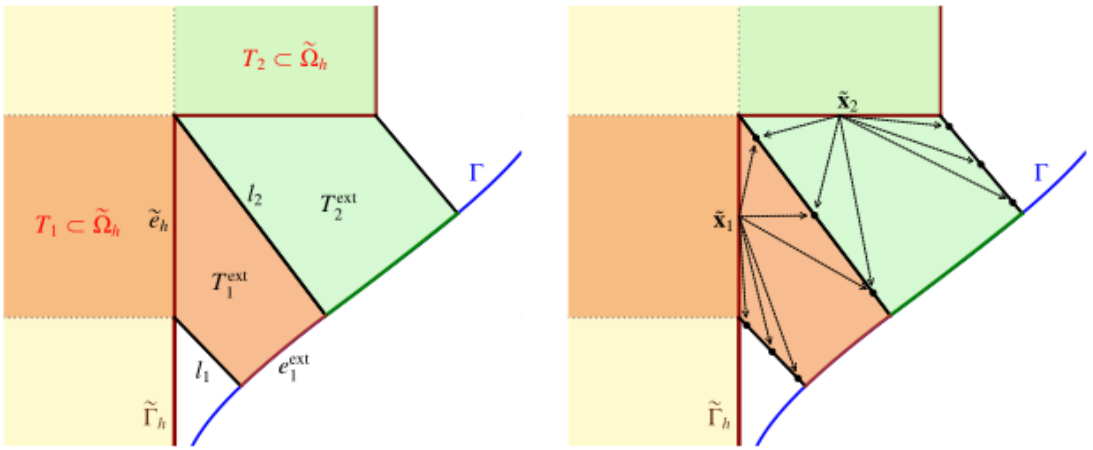

Figure 10. *Left: Main geometric entities of two adjacent gap elements. Right: Quadrature points on the interfaces of the gap elements and their projection from the corresponding surrogate reference point. The arrows indicate the direction of the Taylor expansion used to extend the basis functions to the interface quadrature points.*

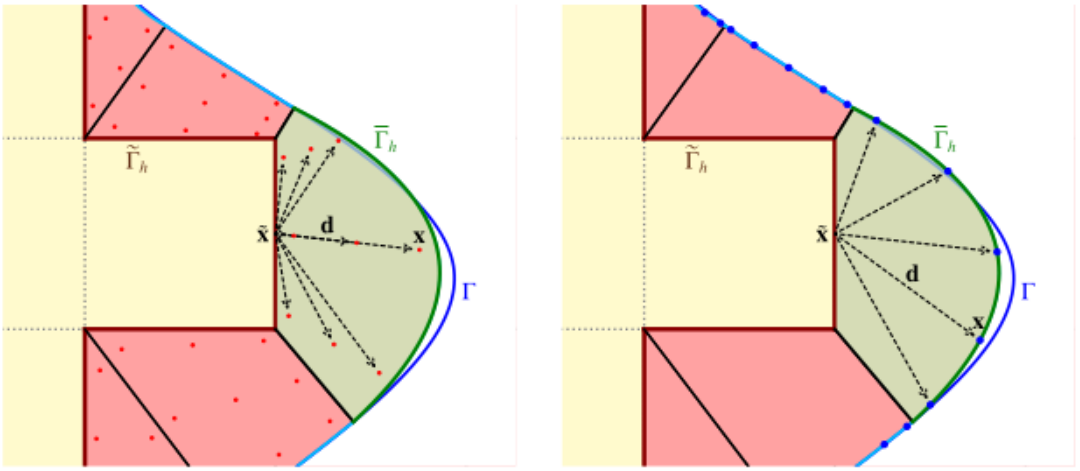

Figure 11. *Left: Extension of basis functions used for integration over the interior of the gap element. Right: Extension of basis functions used for the integration of boundary condition terms on the approximated boundary. Arrows indicate the direction of the Taylor expansion used to evaluate the basis functions at interior and boundary quadrature points.*

From a geometric point of view, the method starts from an internal surrogate domain, obtained by activating only the background elements fully contained inside the physical domain. This choice defines an external gap region between the surrogate boundary and the true boundary. For each edge of the surrogate boundary, the corresponding points on the true boundary are identified by closest-point projection, and the strip enclosed between the surrogate edge and its image on the true geometry is interpreted as a gap element. The collection of these gap elements provides a geometrically consistent approximation of the missing portion of the physical domain. A schematic representation of this workflow is shown in Figure 12, which illustrates the successive construction of the surrogate boundary, gap elements, and quadrature points.

A central ingredient of the formulation is the extension of the active spline approximation into the gap region. For each quadrature point inside a gap element, the corresponding point on the surrogate boundary is identified, and the discrete basis functions are extended by means of a high-order Taylor expansion. In contrast to the standard directional shift used in the classical SBM, the present formulation adopts an enhanced shift operator that retains the relevant mixed derivatives of the spline basis. This is particularly important in tensor-product spline spaces, where mixed terms cannot in general be neglected without losing consistency. The same extension is applied not only to the solution field, but also to its gradients, which is essential for the accurate reconstruction of Neumann fluxes. Since the extension acts only on the existing surrogate basis functions, no additional degrees of freedom are introduced, and the size of the algebraic system remains unchanged. The enhanced operator is defined as:

$$\widetilde{\mathbb{S}}^{p}_{\mathbf{d}}\left(N_A(\tilde{\mathbf{x}})\right) := \sum_{0 \leqslant \alpha_x, \alpha_y \leqslant p} \frac{D^{(\alpha_x,\alpha_y)} N_A(\tilde{\mathbf{x}})}{\alpha_x!\,\alpha_y!}\, d_x^{\alpha_x} d_y^{\alpha_y},$$

where $d = (d_x, d_y)$, $D^{(\alpha_x,\alpha_y)} = \partial^{\alpha_x}_x \partial^{\alpha_y}_y$ denotes the standard multi-index power.

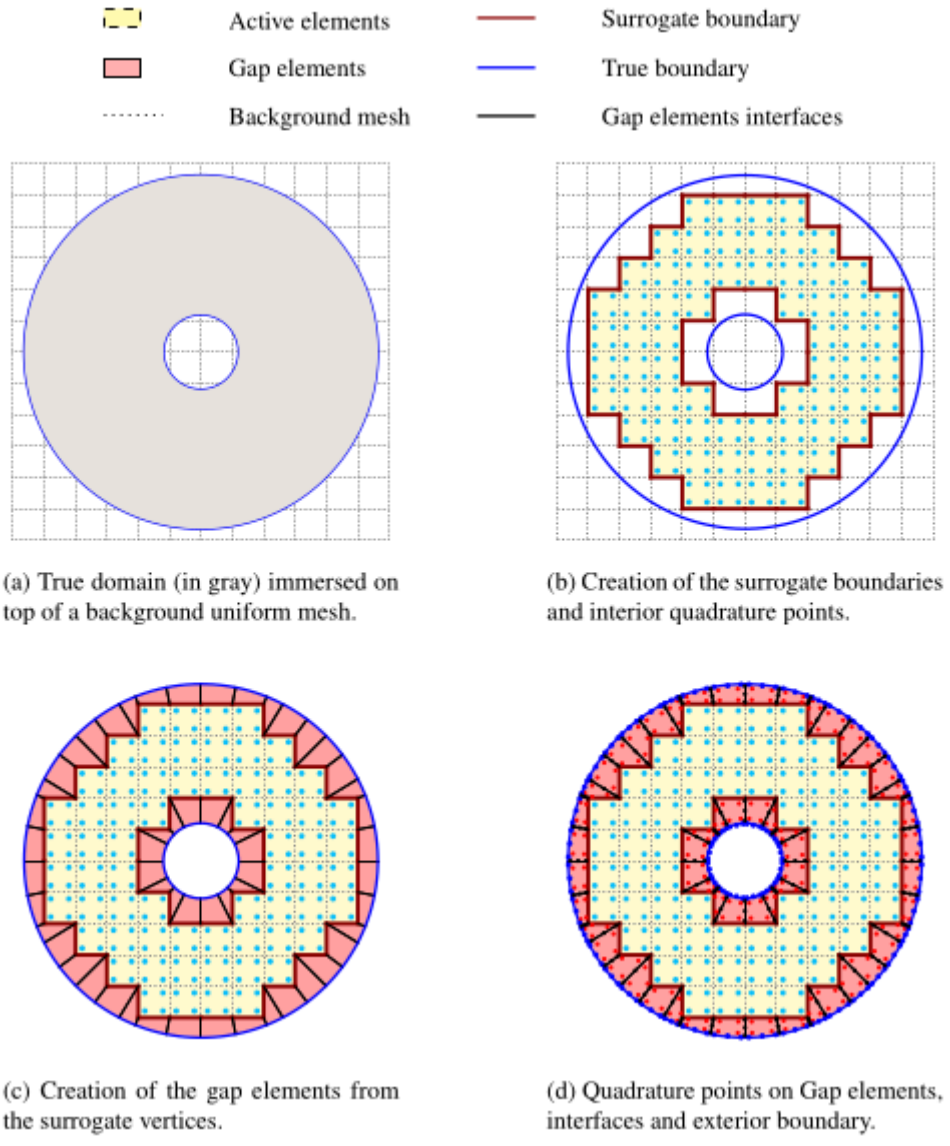

Figure 12. *Visualization of the Gap-SBM for B-splines of order p = 1.*

The numerical integration over the gap region is performed through curvilinear gap elements constructed by means of Coons patch parametrizations. The coons patch mapping F is defined

as

$$\boldsymbol{F}(\xi,\eta) = (1-\eta)\boldsymbol{B}_0(\xi) + \eta\boldsymbol{B}_1(\xi) + (1-\xi)\boldsymbol{L}_0(\eta) + \xi\boldsymbol{L}_1(\eta) - \Big[(1-\xi)(1-\eta)\boldsymbol{P}_{00} + \xi(1-\eta)\boldsymbol{P}_{10} + (1-\xi)\eta\boldsymbol{P}_{01} + \xi\eta\boldsymbol{P}_{11}\Big]$$

where $B_0(\xi)$, $B_1(\xi)$, $L_0(\eta)$, $L_1(\eta)$ are the lower, upper, left, and right boundary curves respectively, with $\xi, \eta \in [0,1]$. By construction the mapping interpolates exactly the four boundary curves as well as the corner points of the quadrilateral.

This choice is particularly natural because each gap element is bounded by three straight edges and one curved edge lying on the true boundary. The Coons construction provides a smooth transfinite interpolation of the element interior and allows standard Gaussian quadrature rules to be used on a reference domain. In practice, the true boundary is approximated locally by a polynomial curve of degree consistent with the spline discretization, so that the geometry of the gap elements remains compatible with the approximation order of the method. Figure 13 is useful here to show how the curvilinear parametrization evolves with the polynomial order.

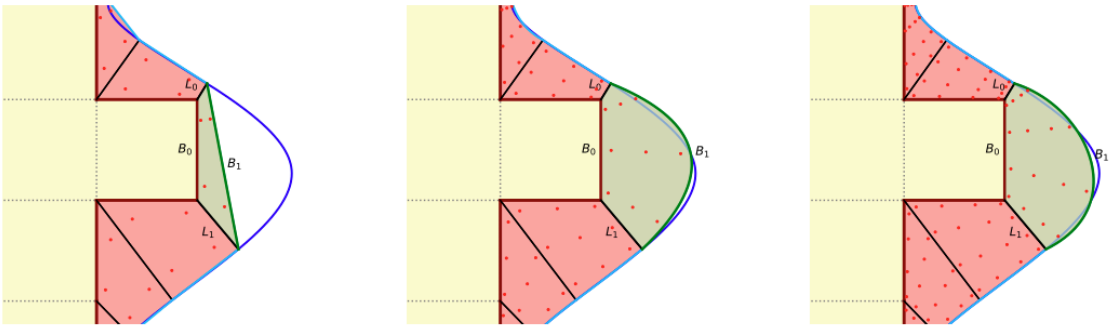

(a) Linear gap element. (b) Quadratic gap element. (c) Cubic gap element.

Figure 13. *Coons patch parametrization and quadrature points for gap elements of increasing polynomial order.*

Another important aspect of the method is that the treatment of the gap region and the treatment of the boundary conditions are conceptually separated. Once the computational domain has been reconstructed through the gap elements, boundary data can be imposed in different ways on the approximated boundary. In addition to direct imposition, the work investigates interpolation-based transfer from the true boundary and an SBM-type extrapolation from the reconstructed boundary to the exact one (see Figure 14). This separation is useful because it makes it possible to distinguish the effect of geometric approximation from the effect of boundary-data transfer, and therefore to understand more clearly where the remaining error comes from when the geometry is only approximated.

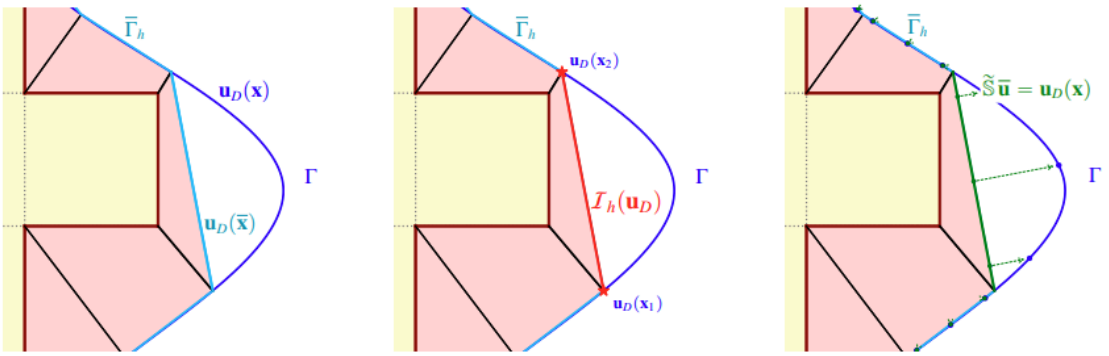

Figure 14. *: Imposition of Dirichlet boundary conditions when the computational boundary does not coincide with the true boundary. From left to right: direct enforcement of the prescribed data on the approximated boundary; enforcement through interpolation of the boundary data sampled on the true boundary Γ; enforcement via the classical Shifted Boundary Method, in which the prescribed boundary data are transferred from Γ to the approximated boundary through the shift operator.*

3.1 Numerical Results

The performance of the proposed Gap–SBM has been assessed through a set of numerical experiments designed to evaluate its accuracy, robustness, and computational properties. Particular attention has been devoted to three aspects that are especially relevant for the present work: the treatment of boundary conditions on curvilinear embedded geometries, the additional computational cost introduced by the gap reconstruction, and the conditioning of the resulting linear systems. Together, these tests provide a synthetic but representative picture of the method: on the one hand, they show that the Gap–SBM restores the accuracy lost by the classical SBM in the presence of Neumann boundary conditions; on the other hand, they confirm that this improvement is achieved without compromising the favorable numerical properties that make shifted-boundary approaches attractive in immersed settings.

The first relevant test is the curvilinear embedded benchmark defined by two concentric circles immersed in a square background domain, with Dirichlet conditions prescribed on the inner boundary and Neumann conditions on the outer one (Figure 12). This example is particularly useful because the geometry is not exactly represented by the computational domain, so that the results directly reflect both the quality of the gap reconstruction and the effect of the boundary-condition treatment. In this setting, the comparison between direct imposition, interpolation-based transfer, and SBM extrapolation shows that all Gap–SBM variants recover the expected asymptotic convergence rates and lead to a substantial improvement in both accuracy and robustness with respect to the classical SBM.

More specifically, the results in Figure 15 show that the influence of the boundary-data treatment depends on the polynomial degree. For linear discretizations, direct imposition already preserves the correct convergence rates, but interpolated boundary conditions and SBM extrapolation provide a visible gain in accuracy, with almost indistinguishable performance. For quadratic discretizations, the geometric approximation improves so rapidly that the differences between the three approaches become almost negligible. For cubic discretizations, the role of the boundary treatment becomes relevant again: while direct imposition remains asymptotically optimal, both interpolation and especially SBM extrapolation improve the solution accuracy at finer resolutions. In this sense, the benchmark highlights an important practical point: once the gap region is accurately reconstructed, the way boundary data are transferred to the approximated boundary can become the dominant factor controlling the final error.

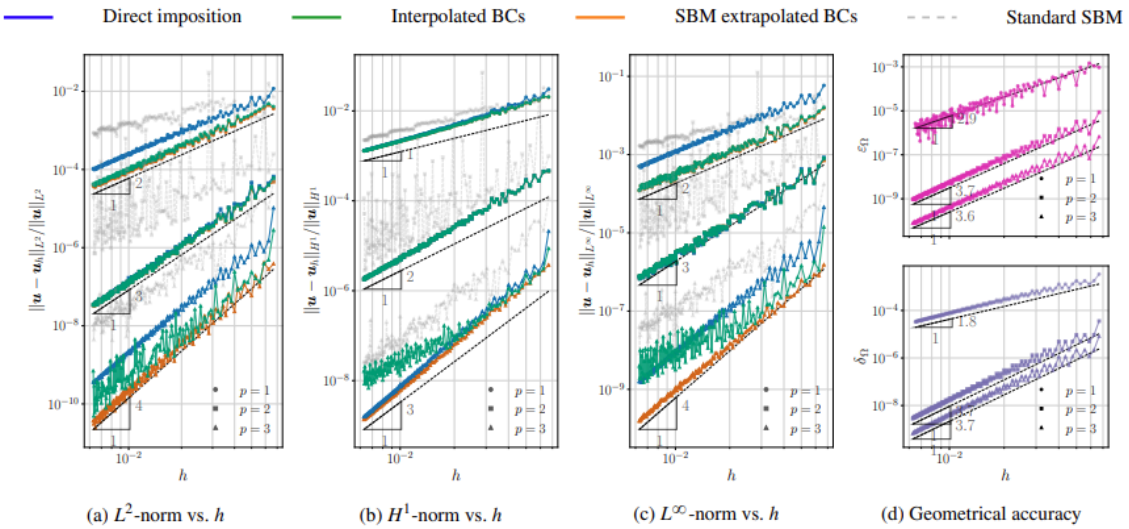

Figure 15. *:Step-by-step convergence study for the concentric-circles benchmark with Dirichlet boundary conditions on the inner circle and Neumann boundary conditions on the outer circle (see Fig. 12). Panels (a)–(c) report the relative solution errors in the L 2 , H 1 , and L inf norms for different boundary-condition treatments. Panel (d) reports geometric error indicators of the surrogate domain.*

The computational-cost analysis confirms that the improved accuracy of the Gap–SBM is obtained with a limited and well-controlled overhead. The timings are split into preprocessing, assembly, and solver stages (see Figure 16). The results show that the assembly cost grows approximately linearly with the number of degrees of freedom, whereas the linear solver cost grows superlinearly and rapidly becomes the dominant contribution under mesh refinement. By contrast, the additional overhead associated with the Gap–SBM construction follows a much milder growth, consistent with the theoretical estimate based on the number of cut surrogate edges. In practice, this means that the extra geometric work required to build and integrate the gap region does not become the dominant part of the simulation as the mesh is refined.

An important practical implication of these results is that the extra cost introduced by the Gap–SBM remains asymptotically of lower order than the cost of solving the linear system. Therefore, although the method requires a more elaborate preprocessing stage than the classical SBM, this additional effort is offset by the fact that the dominant computational burden still lies in the solver, exactly as in standard discretizations. It is also worth noting that, for very coarse linear meshes, the preprocessing stage may appear comparatively large; however, this should be interpreted with care, since both the surrogate-boundary construction and the generation of the gap elements follow a naturally parallelizable workflow. Overall, the timing results indicate that the method achieves a favorable balance between improved accuracy and computational overhead.

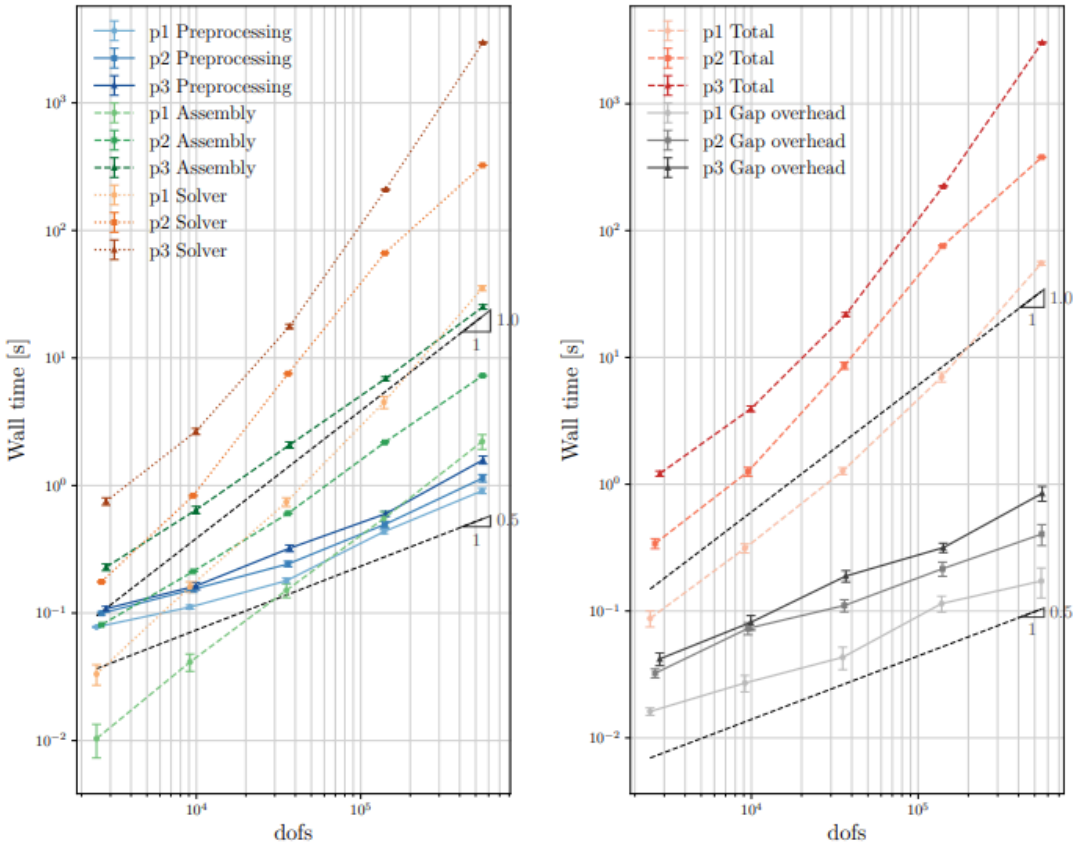

(a) Preprocessing, assembly, and solver costs for $p = 1, 2, 3$.

(b) Total wall time versus additional Gap–SBM overhead for $p = 1, 2, 3$.

Figure 16. *:Computational cost analysis for the circular benchmark problem. The reported times are averaged over 20 repeated simulations.*

The condition-number analysis addresses one of the main motivations behind the Gap–SBM formulation, namely the preservation of robust linear-system behavior in an immersed high-order setting. The comparison with unstabilized cut-integration approaches is particularly informative. In the reported tests, the IBRA formulation without ghost-penalty stabilization exhibits the typical exponential growth of the condition number, together with large oscillations and extreme peaks. By contrast, both the classical SBM and the Gap–SBM display the expected algebraic growth proportional to h^{-2}, confirming that the small cut-cell instability is avoided. Most importantly, the Gap–SBM shows an even smoother and more regular behavior than the classical SBM, with significantly reduced oscillations under mesh refinement.

This result is especially relevant because it shows that integrating over the geometric gap does not destroy the favorable conditioning mechanism inherited from SBM formulations. Even though the Gap–SBM introduces additional coupling terms through the gap contributions, no extra degrees of freedom are added, and all quantities are projected onto the already active basis functions. As a consequence, the stiffness matrix retains the conditioning properties expected from standard isogeometric discretizations. In practical terms, this makes the method much more attractive than cut-integration approaches for large-scale computations, since it supports the use of fast iterative solvers without requiring the additional stabilization machinery typically needed in unfitted methods based on trimmed cells.

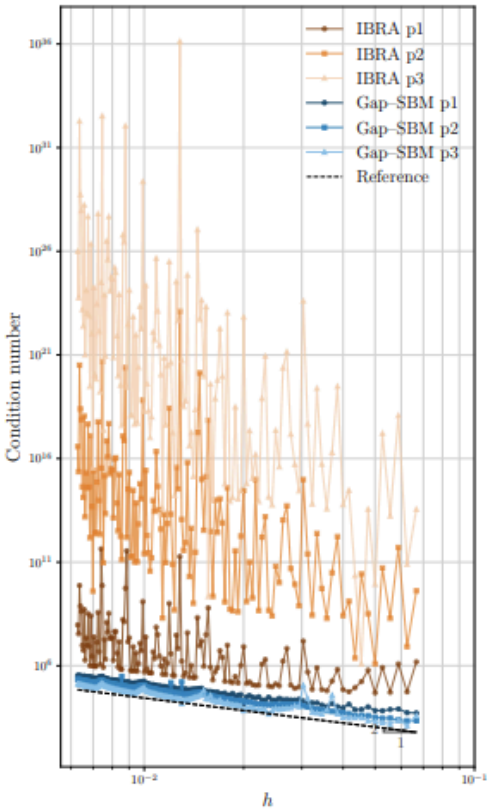

(a) IBRA vs. Gap–SBM

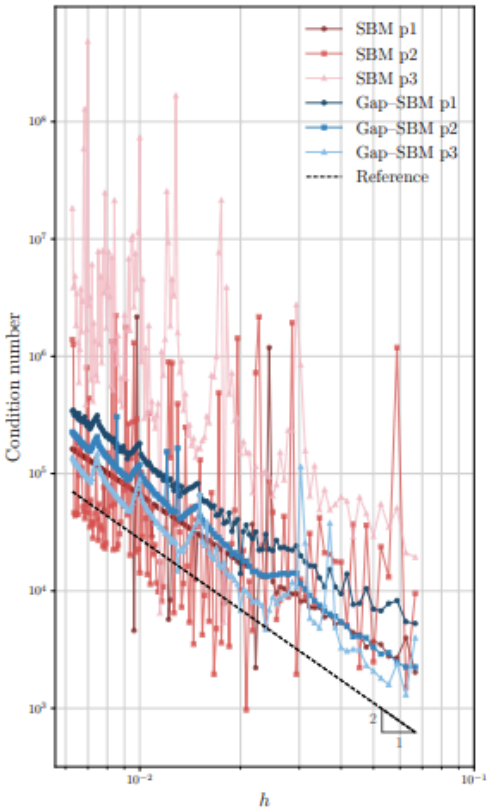

(b) SBM vs. Gap–SBM

Figure 17. *:Condition number as a function of the mesh size for the circular geometry shown in Fig. 12*

4. Extra: THE GAP-SBM FOR MULTIPATCH COUPLING

The technology described above has also proven particularly useful for flexible multipatch coupling in the context of IGA. The reader is referred to [50] for the complete derivation. In the present report, however, we only emphasize the main benefit that this development may bring to immersed contact analysis, namely the possibility of introducing local refinement, either in hhh or in ppp, in the vicinity of immersed boundaries while preserving a consistent global discretization. This is especially relevant for future contact applications, where higher resolution may be required only in localized regions close to the contact interface. An example is shown in Figure 18, where two local patches are introduced to isolate the immersed boundary from the rest of the domain in a Poisson problem with Neumann boundary conditions on the internal boundary, imposed through the classical SBM. The comparison illustrates how such a multipatch setting can be used to improve the local accuracy in a simple and flexible way.

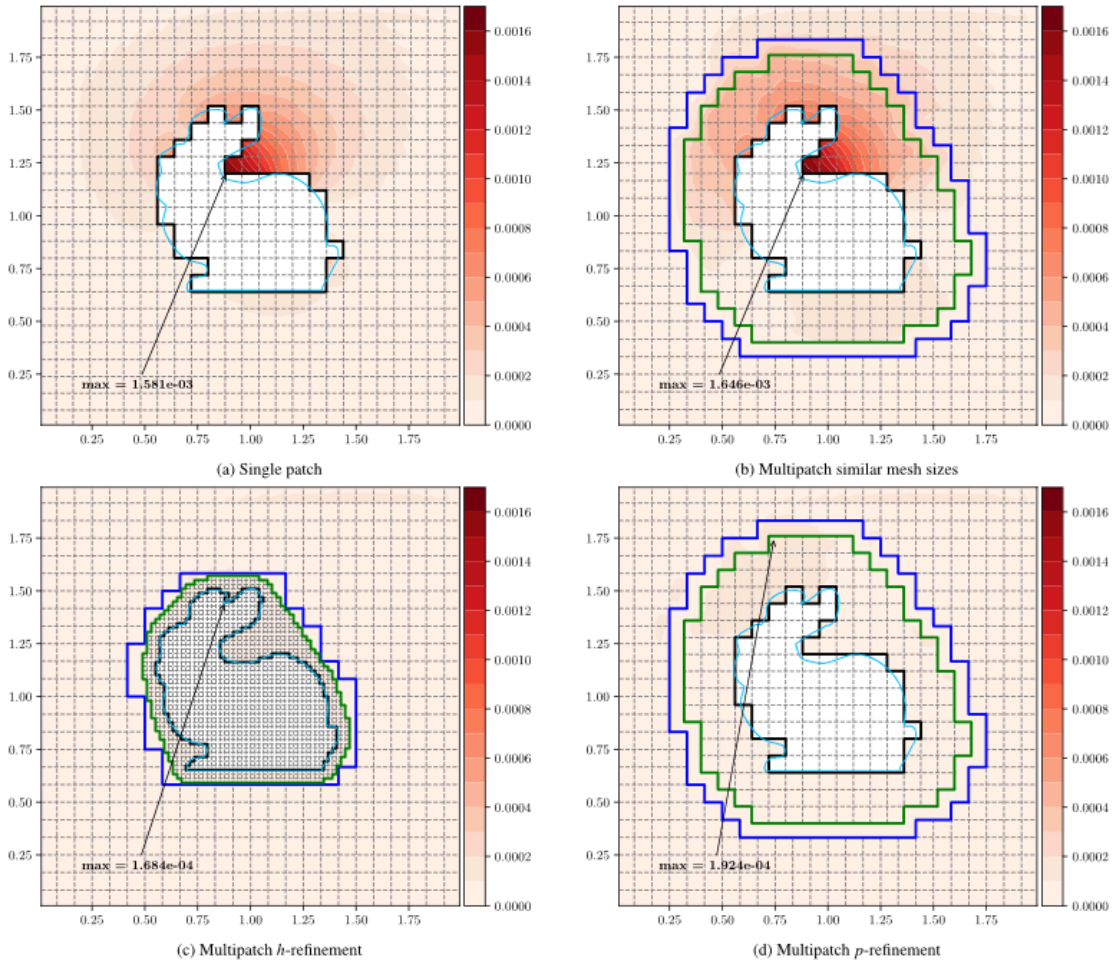

(a) Single patch (b) Multipatch similar mesh sizes

(c) Multipatch h-refinement (d) Multipatch p-refinement

Figure 18. *:Comparison of error distributions for an embedded Neumann boundary (pointwise absolute error). The black solid line represents the surrogate Neumann boundary. The blue line shows the outer patch's surrogate inner boundary, and the green line shows the refined patch's surrogate outer boundary (which coincides with the coupling interface). (a) Single-patch configuration using the classical SBM. (b) Two-patch configuration with similar mesh sizes. (c) Two-patch configuration with local h-refinement around the Neumann boundary (inner patch mesh size reduced by a factor of 4). (d) Two-patch configuration with local p-refinement on the inner patch (cubic polynomial degree in inner patch, vs. quadratic in outer patch). (For interpretation of the references to colour in this figure legend, the reader is referred to the web version of this article.)*

5. CONCLUSIONS AND OUTLOOK

This report presented the current state of the PhD project on immersed and high-order computational mechanics based on the Shifted Boundary Method (SBM) and Isogeometric Analysis (IGA). Starting from the initial integration of SBM within IGA, the work has progressively evolved from a proof of concept for immersed high-order analysis toward a broader framework aimed at combining geometric flexibility, accurate boundary treatment, and robust numerical performance for structural and contact mechanics applications.

A first important outcome is the validation of the SBM in the IGA setting, where the method has been shown to preserve the main advantages of immersed formulations while retaining the accuracy and smooth approximation properties typical of spline-based discretizations. In particular, the previous results confirmed that the classical SBM can effectively handle complex geometries with reduced preprocessing effort, although its treatment of Neumann boundary conditions remains one of its main limitations.

A second outcome, developed in collaboration with Kangan Li and Guglielmo Scovazzi, is the extension of the SBM to frictionless immersed contact in linear elasticity. The results summarized in this report show that contact conditions can be consistently imposed on surrogate contact surfaces, avoiding cut-cell integration and maintaining robustness even in complex and non-watertight geometries. At present, however, this contribution has been achieved in the FEM setting and should therefore be regarded as an important intermediate step toward the final objective of high-order immersed contact in IGA.

The central methodological contribution of the current stage of the project is the development of the high-order isogeometric Gap–SBM. By explicitly reconstructing the geometric strip between the surrogate and true boundaries through high-order Taylor extensions and curvilinear gap elements, the method overcomes the main accuracy limitation of the classical SBM for Neumann boundary conditions. The numerical results show that the Gap–SBM restores optimal convergence, remains only weakly sensitive to the surrogate-boundary position, introduces a limited computational overhead, and preserves the favorable conditioning properties that make shifted-boundary approaches attractive in immersed settings.

A further relevant development is the multipatch coupling strategy derived from the Gap–SBM framework. Although this should be regarded mainly as a supporting tool in the context of the present project, it is particularly promising because it enables robust coupling between

nonconforming patches and provides a flexible mechanism for local h- and p-refinement near immersed boundaries. This capability is expected to play an important role in the next phase of the research, especially for the comparison between classical SBM and Gap–SBM in immersed contact and for future extensions toward nonlinear constitutive behavior.

Overall, the results collected in this report show a clear evolution of the project toward a unified framework in which immersed contact, accurate Neumann treatment, and local refinement strategies can be progressively combined. The next steps will therefore focus on extending immersed contact to the high-order isogeometric setting, comparing classical SBM and Gap–SBM formulations in contact problems, and investigating the same methodologies in the presence of nonlinear materials and plasticity, with the long-term aim of addressing contact problems involving more complex physical behaviors.

6. REFERENCES

[1] Thomas J.R. Hughes, John A. Cottrell, Yuri Bazilevs, Isogeometric analysis: CAD, finite elements, NURBS, exact geometry and mesh refinement, Comput. Methods Appl. Mech. Engrg. 194 (39) (2005) 4135–4195.

[2] John A. Cottrell, Alessandro Reali, Yuri Bazilevs, Thomas J.R. Hughes, Isogeometric analysis of structural vibrations, Comput. Methods Appl. Mech. Engrg. 195 (41) (2006) 5257–5296.

[3] Yuri Bazilevs, Lourenco Beirao da Veiga, John A. Cottrell, Thomas J.R. Hughes, Giancarlo Sangalli, Isogeometric analysis: Approximation, stability and error estimates for h-refined meshes, Math. Models Methods Appl. Sci. 16 (07) (2006) 1031–1090.

[4] Yuri Bazilevs, Victor M. Calo, Yongjie Zhang, Thomas J.R. Hughes, Isogeometric fluid–structure interaction analysis with applications to arterial blood flow, Comput. Mech. 38 (4) (2006) 310–322.

[5] Yongjie Zhang, Yuri Bazilevs, Samrat Goswami, Chandrajit L. Bajaj, Thomas J.R. Hughes, Patient-specific vascular NURBS modeling for isogeometric analysis of blood flow, Comput. Methods Appl. Mech. Engrg. 196 (29) (2007) 2943–2959.

[6] John A. Cottrell, Thomas J.R. Hughes, Alessandro Reali, Studies of refinement and continuity in isogeometric structural analysis, Comput. Methods Appl. Mech. Engrg. 196 (41) (2007) 4160–4183.

[7] Josef Kiendl, Kai-Uwe Bletzinger, Johannes Linhard, Roland Wüchner, Isogeometric shell analysis with Kirchhoff–Love elements, Comput. Methods Appl. Mech. Engrg. 198 (49) (2009) 3902–3914.

[8] David J. Benson, Yuri Bazilevs, Ming-Chen Hsu, Thomas J.R. Hughes, Isogeometric shell analysis: The Reissner–Mindlin shell, Comput. Methods Appl. Mech. Engrg. 199 (5) (2010) 276–289, Computational Geometry and Analysis.

[9] Kenji Takizawa, Yuri Bazilevs, Tayfun E. Tezduyar, Ming-Chen Hsu, Takuya Terahara, Computational cardiovascular medicine with isogeometric analysis, J. Adv. Eng. Comput. 6 (3) (2022) 167–199.

[10] Massimo Carraturo, Carlotta Giannelli, Alessandro Reali, Rafael Vázquez, Suitably graded THB-spline refinement and coarsening: Towards an adaptive isogeometric analysis of additive manufacturing processes, Comput. Methods Appl. Mech. Engrg. 348 (2019) 660–679.

[11] Carlotta Giannelli, Bert Jüttler, Hendrik Speleers, THB-splines: The truncated basis for hierarchical splines, Comput. Aided Geom. Design 29 (7) (2012) 485–498, Geometric Modeling and Processing 2012.

[12] Dominik Schillinger, Luca Dedè, Michael A. Scott, John A. Evans, Michael J. Borden, Ernst Rank, Thomas J.R. Hughes, An isogeometric design-through-analysis methodology based on adaptive hierarchical refinement of NURBS, immersed boundary methods, and T-spline CAD surfaces, Comput. Methods Appl. Mech. Engrg. 249–252 (2012) 116–150, Higher Order Finite Element and Isogeometric Methods.

[13] Martin Ruess, Dominik Schillinger, Yuri Bazilevs, Vasco Varduhn, Ernst Rank, Weakly enforced essential boundary conditions for NURBS-embedded and trimmed NURBS geometries on the basis of the finite cell method, Internat. J. Numer. Methods Engrg. 95 (10) (2013) 811–846.

[14] Jamshid Parvizian, Alexander Düster, Ernst Rank, Finite cell method: h-and p-extension for embedded domain problems in solid mechanics, Comput. Mech. 41 (1) (2007) 121–133.

[15] Ernst Rank, Martin Ruess, Stefan Kollmannsberger, Dominik Schillinger, Alexander Düster, Geometric modeling, isogeometric analysis and the finite cell method, Comput. Methods Appl. Mech. Engrg. 249–252 (2012) 104–115.

[16] Michael Breitenberger, Andreas Apostolatos, Philipp Bucher, Roland Wüchner, Kai-Uwe Bletzinger, Analysis in computer aided design: Nonlinear isogeometric B-Rep analysis of shell structures, Comput. Methods Appl. Mech. Engrg. 284 (2015) 401–457, Isogeometric Analysis Special Issue.

[17] Tobias Teschemacher, Anna M. Bauer, Thomas Oberbichler, Micheal Breitenberger, Riccardo Rossi, Roland Wüchner, Kai-Uwe Bletzinger, Realization of CAD-integrated shell simulation based on isogeometric B-Rep analysis, Adv. Model. Simul. Eng. Sci. 5 (2018) 1–54.

[18] Tobias Teschemacher, Anna M. Bauer, Ricky Aristio, Manuel Meßmer, Roland Wüchner, Kai-Uwe Bletzinger, Concepts of data collection for the CAD-integrated isogeometric analysis, Eng. Comput. 38 (6) (2022) 5675–5693.

[19] Manuel Meßmer, Tobias Teschemacher, Lukas F. Leidinger, Roland Wüchner, Kai-Uwe Bletzinger, Efficient CAD-integrated isogeometric analysis of trimmed solids, Comput. Methods Appl. Mech. Engrg. 400 (2022) 115584.

[20] Manuel Meßmer, Stefan Kollmannsberger, Roland Wüchner, Kai-Uwe Bletzinger, Robust numerical integration of embedded solids described in boundary representation, Comput. Methods Appl. Mech. Engrg. 419 (2024) 116670.

[21] Erik Burman, Ghost penalty, C. R. Math. 348 (21–22) (2010) 1217–1220.

[22] Santiago Badia, Eric Neiva, Francesc Verdugo, Linking ghost penalty and aggregated unfitted methods, Comput. Methods Appl. Mech. Engrg. 388 (2022) 114232.

[23] Alex Main, Guglielmo Scovazzi, The shifted boundary method for embedded domain computations. Part I: Poisson and Stokes problems, J. Comput. Phys. 372 (2018) 972–995.

[24] Alex Main, Guglielmo Scovazzi, The shifted boundary method for embedded domain computations. Part II: Linear advection–diffusion and incompressible Navier–Stokes equations, J. Comput. Phys. 372 (2018) 996–1026.

[25] Nabil M. Atallah, Guglielmo Scovazzi, Nonlinear elasticity with the shifted boundary method, Comput. Methods Appl. Mech. Engrg. 426 (2024) 116988.

[26] Efthymios N. Karatzas, Giovanni Stabile, Leo Nouveau, Guglielmo Scovazzi, Gianluigi Rozza, A reduced-order shifted boundary method for parametrized incompressible Navier–Stokes equations, Comput. Methods Appl. Mech. Engrg. 370 (2020) 113273.

[27] Nabil M. Atallah, Claudio Canuto, Guglielmo Scovazzi, The second-generation shifted boundary method and its numerical analysis, Comput. Methods Appl. Mech. Engrg. 372 (2020) 113341.

[28] Nabil M. Atallah, Claudio Canuto, Guglielmo Scovazzi, Analysis of the shifted boundary method for the Poisson problem in domains with corners, Math. Comp. 90 (331) (2021) 2041–2069.

[29] Antonelli, N., Aristio, R., Gorgi, A., Zorrilla, R., Rossi, R., Scovazzi, G., & Wüchner, R. (2024). The Shifted Boundary Method in Isogeometric Analysis. *Computer Methods in Applied Mechanics and Engineering*, *430*, 117228.

[30] Hertz, Heinrich. "The contact of elastic solids." *J Reine Angew, Math* 92 (1881): 156-171.

[31] Johnson, Kenneth Langstreth. *Contact mechanics*. Cambridge university press, 1987.

[32] Jackson, R. L., & Green, I. (2003, January). A finite element study of elasto-plastic hemispherical contact. In *International Joint Tribology Conference* (Vol. 37068, pp. 65-72).

[33] Barber, J. R., & Ciavarella, M. (2000). Contact mechanics. *International Journal of solids and structures*, *37*(1-2), 29-43.

[34] Wriggers, Peter. *Computational contact mechanics*. Ed. Tod A. Laursen. Vol. 2. Berlin: Springer, 2006.

[35] Kogut, L., & Etsion, I. (2002). Elastic-plastic contact analysis of a sphere and a rigid flat. *J. Appl. Mech.*, *69*(5), 657-662.

[36] Cottrell, J. A., Hughes, T. J., & Bazilevs, Y. (2009). *Isogeometric analysis: toward integration of CAD and FEA*. John Wiley & Sons.

[37] Temizer, I., Wriggers, P., & Hughes, T. (2011). Contact treatment in isogeometric analysis with NURBS. *Computer Methods in Applied Mechanics and Engineering*, *200*(9-12), 1100-1112.

[38] De Lorenzis, L., Temizer, İ., Wriggers, P., & Zavarise, G. (2011). A large deformation frictional contact formulation using NURBS-based isogeometric analysis. *International Journal for Numerical Methods in Engineering*, *87*(13), 1278-1300.

[39] Alart, P., & Curnier, A. (1991). A mixed formulation for frictional contact problems prone to Newton like solution methods. *Computer methods in applied mechanics and engineering*, *92*(3), 353-375.

[40] Kim, J. Y., & Youn, S. K. (2012). Isogeometric contact analysis using mortar method. *International Journal for Numerical Methods in Engineering*, *89*(12), 1559-1581.

[41] Dimitri, R., De Lorenzis, L., Scott, M. A., Wriggers, P., Taylor, R. L., & Zavarise, G. (2014). Isogeometric large deformation frictionless contact using T-splines. *Computer methods in applied mechanics and engineering*, *269*, 394-414.

[42] Puso, M. A., & Laursen, T. A. (2004). A mortar segment-to-segment frictional contact method for large deformations. *Computer methods in applied mechanics and engineering*, *193*(45-47), 4891-4913.

[43] Temizer, I., & Hesch, C. (2016). Hierarchical NURBS in frictionless contact. *Computer Methods in Applied Mechanics and Engineering*, *299*, 161-186.

[44] Dimitri, R. (2015). Isogeometric treatment of large deformation contact and debonding problems with T-splines: a review. *Curved and Layered Structures*, *2*(1).

[45] Atallah, N. M., Canuto, C., & Scovazzi, G. (2021). The shifted boundary method for solid mechanics. *International Journal for Numerical Methods in Engineering*, *122*(20), 5935-5970.

[46] Main, A., & Scovazzi, G. (2018). The shifted boundary method for embedded domain computations. Part II: Linear advection–diffusion and incompressible Navier–Stokes equations. *Journal of Computational Physics*, *372*, 996-1026.

[47] Li, Kangan, et al. "The shifted boundary method for contact problems." *Computer Methods in Applied Mechanics and Engineering* 440 (2025): 117940.

[48] Popp, Alexander, Michael W. Gee, and Wolfgang A. Wall. "A finite deformation mortar contact formulation using a primal–dual active set strategy." *International Journal for Numerical Methods in Engineering* 79.11 (2009): 1354-1391.

[49] Gorgi, Andrea, et al. "The Isogeometric Gap-Shifted Boundary Method." *Available at SSRN 6179147* (2026).

[50] Antonelli, Nicolò, et al. "Isogeometric multipatch coupling with arbitrary refinement and parametrization using the Gap–Shifted Boundary Method." *Computer Methods in Applied Mechanics and Engineering* 456 (2026): 118913.